ELSEVIER

Catalysis Today 51 (1999) 161–175

CATALYSIS TODAY

Catalytic performance, structure, surface properties and active oxygen species of the fluoride-containing rare earth (alkaline earth)-based catalysts for the oxidative coupling of methane and oxidative dehydrogenation of light alkanes

Hui Lin Wan*, Xiao Ping Zhou, Wei Zheng Weng, Rui Qiang Long, Zi Sheng Chao, Wei De Zhang, Ming Shu Chen, Ji Zhong Luo, Shui Qin Zhou

State Key Laboratory for Physical Chemistry of Solid Surface, Department of Chemistry and Institute of Physical Chemistry, Xiamen University, Xiamen 361005, China

Abstract

The fluoride-containing catalysts, mostly of the rare earth (alkaline earth)-based system, demonstrate good catalytic performances for the oxidative coupling of methane and oxidative dehydrogenation of ethane, propane as well as iso-butane. The results of structural analysis of the catalysts for oxidative coupling of methane show that the promoting effects of the fluoride in the catalysts may be principally related to the phase–phase interaction between fluoride and oxide. Compared to the corresponding alkaline earth oxide promoted rare earth oxide catalyst system, an alkaline earth fluoride-promoted rare earth oxide catalyst system is less basic and will therefore be favorable to reduce CO_2 inhibition in the reaction of methane oxidative coupling. However, there is no simple correlation between the acidity/basicity of a methane oxidative coupling catalyst and its catalytic performance. In the experiments of in situ spectroscopic characterizations carried out at the temperature from 650°C to 800°C, O_2^- species was detected over five fluoride-containing rare earth (alkaline earth)-based catalysts for methane oxidative coupling reaction, and the reactions between O_2^- species and CH_4 to form C_2H_4 and the corresponding side-products were observed using in situ IR over four catalysts, which suggest that O_2^- is probably the active oxygen species for the methane oxidative coupling reaction over the corresponding catalysts.

Keywords: Oxidative coupling of methane; Oxidative dehydrogenation of light alkanes; Fluoride-containing rare earth-based catalysts; Oxygen species; Acid–base properties; *In situ* IR; *In situ* Raman; TPD

1. Introduction

The oxidative coupling of methane (OCM) to make ethylene and the oxidative dehydrogenation of ethane (ODE) and propane (ODP) to make the corresponding olefins are of significance for their potential in effective utilization of natural gas and light alkanes resources. Recently, there have been extensive efforts throughout the world to develop economically feasible catalytic processes for these reactions.

The OCM reaction has been a subject of intensive study since Keller and Bhasin [1] reported their early

*Corresponding author.

0920-5861/99/$ – see front matter
PII: S0920-5861(99)00019-X

work on the reaction in 1982. After more than a decade of study, many catalyst systems have been developed. These include supported transition metal oxide catalyst systems [1–5] partially stabilized with alkali (e.g. MnO_x–Na_2WO_4/SiO_2), reducible non-transition metal oxides catalyst systems [6–11] supported on basic carriers (e.g. PbO_x/MgO), and alkaline earth oxide (AEO) and/or rare earth oxide (REO)-based irreducible metal oxides (and carbonate), mostly of the host–dopant type catalyst systems [12–31]. Many catalysts in the latter system such as Li^+/MgO, Na^+/CaO, Sr^{2+}/La_2O_3 and ThO_2–La_2O_3–AEO–$BaCO_3$ have been intensively investigated. These investigations have come up with some general principles for constituent selection and catalyst design of the OCM catalysts. A lot of catalyst systems such as transition metal complex oxide-based catalysts, e.g. MoVNbSbCaO [32] for ODE, and VMgO system [33] for ODP have also been developed. Besides, there are many experimental evidences indicating that the catalytic property of some OCM and ODE catalysts can be significantly improved by chlorine present either in the form of a chloride component built into the catalyst such as Cl^- promoted Li^+/MgO or as a volatile chlorinated compound (organic or inorganic) in the reactant feed [34–49].

Drawing inspiration from the promoting effect of Cl^-, we considered that it would also be interesting and of fundamental significance to have a detailed investigation on the influence of other halides, especially fluorides since alkaline earth or rare earth fluoride is usually more stable than the corresponding chloride under the reaction conditions. Following this clue, we have developed a series of fluoride-containing rare earth-based catalysts, particularly fluoride-containing rare earth–alkaline earth catalyst systems [50–63] with good catalytic performances for OCM, ODE as well as for ODP reactions. In this review, the catalytic performances of the fluoride-containing catalysts for OCM, ODE, ODP and oxidative dehydrogenation of iso-butane (ODIB) reactions will be reported, with the detailed discussions focused on the nature of structure chemistry of the fluoride-promoted OCM catalysts and the relationship between surface acidity/basicity of the fluoride-containing OCM catalysts and their catalytic properties. The results of in situ spectroscopic characterizations of the active oxygen species such as superoxide (O_2^-) species and its reactivity over several fluoride-containing catalysts for OCM are also presented.

2. Catalytic performances of fluoride-containing rare earth and/or alkaline earth-based catalysts for OCM, ODE, ODP and ODIB reactions

The catalytic performances of a series of alkaline earth fluoride (AEF) promoted REO, oxyfluoride as well as fluoride catalysts are shown in Tables 1–6. The catalysts are SrF_2/La_2O_3 or SrO/LaF_3 [51,52] (Table 1), a series of SrF_2/Ln_2O_3 (Ln=Nd, Sm, Eu, Gd, Dy, Ho, Er, Tm, Yb) [53] (Table 2), BaF_2 modified REO (Ce, Pr, Tb) with variable valence [51,54,59,60] (Table 3) and BaF_2/LaOF catalyst [55,57] (Table 4) for OCM, and BaF_2/LaF_3 [51,58] (Table 5) and BaF_2/LaOF [56,57] (Table 6) for ODE. In the BaF_2/LaF_3 catalysts, LaF_3 is a possible precursor of LaOF and/or La_2O_3, which can be formed when the catalyst was calcinated at ca. ~900°C and hydrolyzed slowly even under very low air humidity [64]. Comparing to the corresponding AEO modified REO catalyst system (Table 1), e.g. SrO/La_2O_3, the catalysts with fluorides (SrF_2/La_2O_3 or SrO/LaF_3) showed better catalytic performance for the OCM reaction. Similar and more remarkable promotion effects can also be observed from the data in Tables 2 and 3, as well as in the AEF (e.g. BaF_2) containing transition metal (Ti, Zr) oxide catalysts [61,62]. In the above mentioned fluoride-containing OCM and ODE catalysts, the BaF_2/LaOF catalysts are prepared based upon the principles of structurally directed constituent selection, i.e. doping the tetragonal LaOF of defective fluorite structure with metal fluoride of lower cationic valence. These catalysts demonstrated good catalytic performance for both the OCM [55,57] and ODE [56,57] reactions. Under the conditions of 770°C and GHSV=15 000 h^{-1} with CH_4/O_2=6 and 9, CH_4 conversions of 19.5% and 16.5% with C_2 selectivities of 81.2% and 84.5% were obtained (Table 4), respectively, over a BaF_2/9LaOF catalyst. In both cases, the sum of CH_4 conversion and C_2 selectivity was over 100%. Over a BaF_2/2.33LaOF catalyst and under the conditions of 640°C and GHSV=11 600 h^{-1} with C_2H_6/O_2=2, C_2H_6 conversion of 80.8% with C_2H_4 selectivity of 70.8% could be achieved (Table 6).

Table 1
Catalytic performance for methane oxidative coupling

Catalyst	Temperature (°C)	Conversion (%)	Selectivity (%)				Yield of C_2 (%)
		CH_4	CO	CO_2	C_2H_4	C_2H_6	
La_2O_3	750	27.1	15.9	53.7	19.0	11.4	8.2
	700	28.4	11.7	51.4	21.5	15.4	10.5
	650	29.3	9.0	47.3	24.6	19.2	12.8
LaF_3	750	2.1	0	46.2	0	53.8	1.1
SrO	750	0.9	0	48.8	0	51.2	0.5
$SrO/4La_2O_3$	750	25.4	6.3	57.6	20.8	15.3	9.2
	700	27.0	3.9	50.6	25.4	20.1	12.3
	650	27.3	0	49.2	28.1	22.7	13.9
SrO/La_2O_3	750	29.5	7.1	44.2	29.4	19.3	14.4
	700	30.2	8.2	40.9	29.2	21.7	15.4
$SrO/4LaF_3$	750	31.8	10.2	35.8	37.8	16.2	17.2
	700	32.0	11.9	31.0	35.7	21.4	18.2
SrO/LaF_3	750	33.8	16.0	30.1	40.0	13.9	18.2
	700	33.7	13.6	29.7	36.2	19.4	19.1
$SrF_2/4La_2O_3$	750	30.5	4.7	44.3	33.2	17.8	15.6
	700	32.5	4.8	40.8	34.0	20.4	17.7
	650	34.7	5.7	36.8	35.8	21.7	19.9
SrF_2/La_2O_3	750	33.9	9.5	33.5	37.9	19.1	19.3
	700	31.9	11.1	31.2	33.4	24.3	18.4

Feed: CH_4:O_2=3:1, no dilution gas, GHSV=15 000 h^{-1}. The data were obtained after 30 min on stream (adapted from Ref. [52]).

Table 2
The catalytic performance for OCM over the rare earth sesquioxides promoted by strontium fluorides

Catalyst	Temperature (°C)	Conversion (%)	Selectivity (%)						Yield of C_2 (%)
		CH_4	O_2	CO	CO_2	C_2H_4	C_2H_6	C_2	
La_2O_3	700	29.4	100	10.5	52.3	21.5	15.7	37.2	10.9
$SrF_2/4La_2O_3$	700	34.2	98.1	6.4	36.3	36.1	21.2	57.3	19.6
Nd_2O_3	750	27.2	99.1	7.2	53.5	20.1	19.2	39.3	10.7
SrF_2/Nd_2O_3	750	34.3	98.9	4.0	38.9	33.1	24.0	57.1	19.6
Sm_2O_3	800	26.3	99.2	8.9	52.3	21.6	17.2	38.8	10.2
SrF_2/Sm_2O_3	800	34.0	99.5	3.9	40.3	33.1	22.7	55.8	19.0
Eu_2O_3	750	26.3	98.4	13.8	53.1	21.8	11.3	33.1	8.7
SrF_2/Eu_2O_3	750	33.1	99.0	6.7	40.4	31.9	21.0	52.9	17.5
Gd_2O_3	750	29.5	99.7	17.5	49.0	20.1	13.4	33.5	9.9
SrF_2/Gd_2O_3	750	34.4	99.5	5.9	39.5	32.0	22.6	54.6	18.8
Dy_2O_3	750	31.3	99.5	12.4	45.0	25.0	17.6	42.6	13.3
SrF_2/Dy_2O_3	750	32.6	96.3	8.5	40.0	32.0	19.5	51.5	16.8
Ho_2O_3	750	28.8	99.3	18.2	48.8	19.9	13.1	33.0	9.5
SrF_2/Ho_2O_3	750	30.8	97.3	8.6	45.5	26.7	19.1	45.8	14.1
Er_2O_3	750	27.6	99.1	13.2	52.4	20.0	14.4	34.4	9.5
SrF_2/Er_2O_3	750	29.3	96.6	10.0	47.1	23.8	19.1	42.9	12.6
Tm_2O_3	750	26.4	99.4	18.2	53.8	16.4	11.6	28.0	7.4
SrF_2/Tm_2O_3	750	28.6	99.5	8.5	51.2	21.2	19.1	40.3	11.5
Yb_2O_3	750	28.8	99.4	20.3	48.5	19.3	11.9	31.2	9.0
SrF_2/Yb_2O_3	750	28.7	99.4	12.7	51.6	19.9	15.8	35.7	10.3

Feed: CH_4:O_2=3:1, no inert gas for dilution, GHSV=20 000 h^{-1}. The data were obtained after 30 min on stream.

Table 3
The catalytic performance for OCM over the reducible rare earth oxides promoted by BaF_2

Catalyst	Conversion (%)	Selectivity (%)						Yield of C_2 (%)
	CH_4	O_2	CO	CO_2	C_2H_4	C_2H_6	C_2	
CeO_2	22.4	99.6	21.5	75.8	1.2	1.6	2.8	0.6
$4BaF_2/CeO_2$	32.3	99.5	2.2	43.2	34.2	20.4	54.6	17. 6
Pr_6O_{11}	23.1	99.5	6.9	71.5	8.2	13.4	21.6	5.0
$12BaF_2/Pr_6O_{11}$	33.5	99.4	3.7	38.8	35.3	22.2	57.5	19.3
Tb_4O_7	24.2	99.5	10.0	67.1	8.5	14.4	22.9	5.5
$8BaF_2/Tb_4O_7$	33.1	99.4	3.9	40.0	35.7	20.4	56.1	18.6

Feed: CH_4:O_2=3:1, no inert gas for dilution, GHSV=20 000 h^{-1}. The data were obtained after 15 min on stream at 800°C (adapted from Ref. [60]).

Table 4
The OCM performance of the BaF_2/LaOF catalysts with different BaF_2 contents[a]

Catalyst	Conversion of CH_4 (%)	Selectivity (%)					Yield of C_2 (%)
		CO	CO_2	C_2H_4	C_2H_6	C_2	
LaOF	25.0	12.6	40.8	27.2	19.4	46.6	11.7
BaF_2/19LaOF	26.4	4.7	38.6	31.9	24.8	56.7	15.0
BaF_2/13.29LaOF	26.8	9.0	32.7	35.5	22.8	58.3	15.6
BaF_2/9LaOF	28.7	3.1	29.6	44.7	22.6	67.3	19.3
BaF_2/9LaOF[b]	19.5	0	18.8	41.2	40.0	81.2	15.8
BaF_2/9LaOF[c]	16.5	0	15.5	23.5	61.0	84.5	13.9
BaF_2/5.67LaOF	27.9	3.0	29.1	43.7	24.2	67.9	18.9
BaF_2/4.56LaOF	27.4	8.2	27.9	40.3	23.6	63.9	17.5
BaF_2/4LaOF	26.9	9.9	27.0	41.6	21.5	63.1	17.0
BaF_2/2.33LaOF	23.8	12.8	28.0	39.0	20.2	59.2	14.1

The data were obtained after 120 min on stream (adapted from Ref. [57]).
[a] Reaction conditions: feed=CH_4:O_2=4:1, temperature=780°C, GHSV=15 000 h^{-1}.
[b] Reaction conditions: feed=CH_4:O_2=6:1, temperature=770°C.
[c] Reaction conditions: feed=CH_4:O_2=9:1, temperature=770°C.

On the basis of developing fluoride-containing OCM and ODE catalysts, a type of alkali-promoted fluoride-containing REO-based catalyst with good catalytic performance for ODP was also prepared [51,65] (Table 7). This catalyst system is one of the best catalyst systems reported so far in the literature for the ODP reaction [65,66]. Under the conditions of 500°C, C_3H_8:O_2:N_2=4:5:11 and GHSV=6000 h^{-1}, we have obtained a propylene yield of 35–36% over 3 wt%Cs_2O/CeO_2–CeF_3 and 3 wt%$Cs_2O/2CeO_2$–CeF_3 catalysts, much higher than the propylene yield over the VMgO system under similar conditions [67].

Table 5
Catalytic performance of LaF_3–BaF_2 catalysts for ODE at 470°C

Catalyst	C_2H_6 conversion (%)	Content of product (%)					C_2H_4 selectivity	C_2H_4 yield (%)
		CO	CO_2	CH_4	C_2H_4	C_2H_6		
$LaF_3/4BaF_2$	46.3	0	0.20	0.43	3.93	4.92	92.7	42.9
LaF_3/BaF_2	46.8	0	0.17	0.71	4.01	5.05	90.2	42.2
$4LaF_3/BaF_2$	54.2	0.42	0.25	0.87	4.05	4.08	84.0	45.5

Feed=C_2H_6:O_2:N_2=10:5:85, GHSV=18 000 h^{-1}. The data were obtained after 30 min on stream (adapted from Ref. [51]).

Table 6
The ODE performance of BaF_2/LaOF catalysts with different BaF_2 contents[a]

Catalyst	Temperature (%)	X_{O_2} (%)[b]	Conversion of C_2H_6 (%)	Selectivity (%)				Yield of C_2H_4 (%)
				CO	CH_4	CO_2	C_2H_4	
Quartz sand	700	31.7	3.0	0	0	25.8	74.2	2.2
	720	30.2	5.2	0	0	20.7	79.3	4.1
LaOF	660	0	44.6	13.3	4.0	24.2	58.5	26.1
BaF_2/15.67LaOF	660	0	54.7	10.3	3.6	17.1	69.0	37.7
BaF_2/11.5LaOF	660	0	55.2	2.9	3.8	19.3	74.0	40.8
BaF_2/9LaOF	660	0	57.8	8.4	4.3	17.6	70.7	40.9
BaF_2/9LaOF[c]	660	0	75.5	11.8	8.6	12.7	66.9	50.5
BaF_2/7.33LaOF	660	0	50.2	8.1	3.1	20.3	68.5	34.4
BaF_2/6.14LaOF	680	0	53.4	9.8	3.6	19.7	66.9	35.7
BaF_2/2.85LaOF	660	0	52.4	9.3	3.5	20.8	66.4	34.8
BaF_2/2.33LaOF	660	0	46.2	8.0	3.5	24.5	64.0	29.6
BaF_2/2.33LaOF[d]	640	0	80.8	8.7	8.8	11.7	70.8	57.2

The data were obtained after 120 min on stream (adapted from Ref. [57]).
[a] Reaction conditions: feed=C_2H_6:O_2=67.7:32.3; GHSV=2700 h^{-1}.
[b] X_{O_2}=the molar percentage of O_2 in the effluent.
[c] GHSV=6000 h^{-1}.
[d] GHSV=11600 h^{-1}.

For the reaction of ODIB, the CeF_3 modified rare earth sesquioxide catalysts also show satisfactory catalytic performance [68] (Table 8). However, under the same reaction conditions, the conversion of ODIB reaction is lower than that of the ODP reaction over the same catalysts (Table 9). This phenomenon may have resulted from that the abstractions of the hydrogen atoms bonded to the tertiary carbon of iso-butane and of those bonded to the secondary carbon of propane may be the rate-limiting steps, respectively, for the alkanes activation, and thus the iso-butane molecule with larger steric hindrance will be more difficult than the smaller propane molecule to make the active sites of the catalyst accessible, in spite of the fact that the corresponding C–H bond energy of iso-butane (∼91 kcal/mol) is smaller than that of propane (∼95 kcal/mol).

3. Structure aspects of the fluoride-promoted catalyst and the principal nature of the promoting effects of fluoride

X-ray diffraction (XRD) experiments have detected the formation of new phases in more than 10 fluoride-containing rare earth–alkaline earth as well as alkaline earth–transition metal oxide-based catalyst systems. For example, SrF_2 and the LaOF phases with tetra-

Table 7
Catalytic performance of catalysts for oxidative dehydrogenation of propane at 500°C

Catalyst	C_3H_8 conversion (%)	Selectivity (%)						C_3H_6 yield (%)
		C_3H_6	CH_4	C_2H_6	C_2H_4	CO_2	CO	
CeO_2	86.7	7.9	39.8	3.1	23.9	17.8	7.0	6.85
CeO_2-2CeF_3	10.3	72.7	0	0	0	13.2	14.0	7.49
3 wt%Cs_2O/2CeO_2-CeF_3	53.4	67.5	3.5	0	12.2	1.3	3.4	36.0
3 wt%Cs_2O/CeO_2-CeF_3	47.5	74.6	3.4	0	16.5	0.5	5.0	35.4
3 wt%Cs_2O/CeO_2-2CeF_3	41.3	81.1	3.8	0	10.7	0.8	3.6	33.5
3 wt%Cs_2O/CeO_2-3CeF_3	7.7	84.4	0	0	0	0	11.6	6.50

Feed=C_3H_8:O_2:N_2=4:5:11, GHSV=6000 h^{-1}. The data were obtained after 120 min on stream (adapted from Ref. [51]).

Table 8
Catalytic performance of catalyst for oxidative dehydrogenation of iso-butane at 500°C

Catalyst	Conversion of iso-butane (%)	Selectivity (%)				Yield of iso-butane (%)
		i-C_4H_8	C_3H_6	C_2H_4	CO+CO_2	
Nd_2O_3/2CeF_3	14.6	74.9	0.42	19.3	5.4	10.9
Sm_2O_3/2CeF_3	13.5	77.0	0.35	17.9	4.8	10.4
La_2O_3/2CeF_3	14.2	68.0	0	14.4	17.6	9.64
Y_2O_3/2CeF_3	15.4	71.3	0.45	18.8	9.5	10.9

Feed=i-C_4H_{10}:O_2=1:1, GHSV=6000 h^{-1}. The data were obtained after 120 min on stream (adapted from Ref. [51]).

Table 9
Comparison of the catalytic performance of rare earth-based catalysts for the oxidative dehydrogenation of propane and iso-butane

Catalyst	Conversion (%)	Selectivity (%)					Yield (%)
	C_3H_8	C_3H_6	CH_4	C_2H_4	CO	CO_2	C_3H_6
Sm_2O_3/4CeF_3	7.5	92.8	0	0	0	7.2	6.96
Nd_2O_3/4CeF_3	8.8	99.0	0	0	0	1.0	8.71
Y_2O_3/4CeF_3	9.0	97.0	0	0	0	3.0	8.7.
	i-C_4H_{10}	i-C_4H_8	CH_4	C_3H_6	CO	CO_2	i-C_4H_8
Sm_2O_3/4CeF_3	5.61	84.7	2.53	6.60	2.87	4.75	3.48
Nd_2O_3/4CeF_3	4.31	87.9	1.45	6.27	1.50	2.87	3.79
Y_2O_3/4CeF_3	6.41	78.6	3.96	14.4	1.50	1.54	5.04

Reaction temperature=500°C, feed=alkane:O_2:N_2=2:3:5, GHSV=6000 h^{-1}. The data were obtained after 120 min on stream.

gonal (tetragonal LnOF is a non-stoichiometric compound and can be expressed by the formula LnO_xF_{3-2x}; the ideal unit cell composition with x being 0.75 is $Ln_4O_3F_6$), rhombohedral and cubic structures were detected in a SrO–LaF_3 catalyst [52] (Table 10). Tetragonal and rhombohedral NdOF [53], tetragonal $Gd_4O_3F_6$ (Table 10), as well as $BaTiOF_4$ and orthorhombic $Ba_3Ti_2O_2F_{10}$ [61] phases were also detected, respectively, in the corresponding SrF_2/Nd_2O_3, AEF (Ca, Sr, Ba) modified gadolinium oxide and BaF_2/TiO_2 catalyst systems. In general, the lanthanide oxyfluorides (LnOF) were found to be one of the main component in many catalysts [51–53]. For some catalysts, such as BaF_2–CeO_2, only the original phases (i.e. BaF_2 and CeO_2) were detected by XRD. Compared to the lattice parameters of the pure BaF_2 and CeO_2, in the BaF_2/CeO_2 catalyst, however, the lattice of BaF_2 phase was slightly contracted while

Table 10
Results of XRD analysis of SrO/LaF_3 and AEF/Gd_2O_3 catalysts

Catalyst	Composition and structure[a]
SrO/4LaF_3	Tetragonal LaOF (s, a=4.091, c=5.837); cubic SrF_2 (w, a=5.800); LaF_3 (w)
SrO/2LaF_3	Rhombohedral LaOF (m, a=7.131, b=32.010); tetragonal LaOF (s); SrF_2 (m); LaF_3
1.22SrO/LaF_3	SrF_2 (s); tetragonal LaOF (s); cubic LaOF (m, a=5.76)
CaF_2/2Gd_2O_3	Cubic Gd_2O_3 (vs, a=10.81); cubic CaF_2 (w, a=5.46); tetragonal $Gd_4O_3F_6$ (vw, a=5.60, c=5.50)
CaF_2/Gd_2O_3	Cubic Gd_2O_3 (vs); cubic CaF_2 (m); tetragonal $Gd_4O_3F_6$ (vw)
4CaF_2/Gd_2O_3	Cubic Gd_2O_3 (vs); cubic CaF_2 (vs); tetragonal $Gd_4O_3F_6$ (w)
4SrF_2/Gd_2O_3	Cubic Gd_2O_3 (vs); cubic SrF_2 (vs, a=5.80); tetragonal $Gd_4O_3F_6$ (w)
4BaF_2/Gd_2O_3	Cubic Gd_2O_3 (vs); cubic BaF_2 (vs, a=6.20); tetragonal $Gd_4O_3F_6$ (vw)

[a] vs=very strong; s=strong; m=medium; w=weak; vw=very weak.

Table 11
Calculation results of lattice expansion and contraction for the BaF_2/CeO_2 catalysts

Catalyst	Lattice	
	CeO_2 (Cubic)	BaF_2 (Cubic)
BaF_2/CeO_2	$a=b=c=5.412$	$a=b=c=6.147(5)$
$2BaF_2/CeO_2$	$a=b=c=5.422$	$a=b=c=6.15601(1)$
$3BaF_2/CeO_2$	$a=b=c=5.438–5.432$	$a=b=c=6.1688–6.192$
$4BaF_2/CeO_2$	$a=b=c=5.431–5.430$	$a=b=c=6.154–6.158$
$5BaF_2/CeO_2$	$a=b=c=5.428–5.430$	$a=b=c=6.169–6.160$
Pure sample	$a=b=c=5.4112$	$a=b=c=6.2001$

that of CeO_2 was slightly expanded (Table 11) [51,54,59]. These results indicated that partially anionic (O^{2-}/F^-) and possibly cationic (e.g. Ba^{2+}/Ce^{4+}) exchanges between the oxide and fluoride phases took place in the catalysts. As a result of ionic exchanges between the oxide and fluoride phases, new phases such as oxyfluorides, and lattice defects such as anionic vacancies (e.g. in the case of substituting O^{2-} for F^- and/or cation with lower valence for cation with higher valence) were formed. It should also be pointed out that the rare earth oxyfluoride (REOF) compound is an ionic conductor with superstructure of fluorite and may contain intrinsic anionic Frenkel defects and anionic vacancies [69]. The presence of anionic vacancies in the oxide or oxyfluoride with stable cation valence may provide suitable sites available for oxygen adsorption, while a catalyst with more anionic vacancies and high anion mobility will be favorable for the migration of surface OH^- group formed by the reaction of the surface active oxygen species with the hydrogen atom of CH_4 molecule to another surface OH^- site, and then elimination as H_2O to regenerate the anionic vacancy.

From the data shown in Table 2, it is interesting to have found that the C_2 yield of SrF_2 promoted Ln_2O_3 catalysts decreased roughly with the increase of atomic number of Ln in the periodic table, i.e. La, Nd>Sm>Eu, Gd>Dy>Ho>Er>Tm>Yb, which is consistent with the successive decrease of the conductivity of rare earth sesquioxides [70]. Since the OCM reaction usually performed at the temperature above 650°C, the cations and/or anions in the oxides may become substantially mobile and the ionic conductivity becomes an important component for the conductivity [69]. This implies that the mobility of lattice oxygen for Ln_2O_3 at high temperature may also decrease in the same sequence. If the amount of LnOF formed (detected by the XRD) in the SrF_2/Ln_2O_3 catalysts is used as a criterion to measure the extent of F^- and O^{2-} exchange between the SrF_2 and Ln_2O_3 phases, it can be found that the extent of anionic exchange between the fluoride and oxide phases also decrease with the increase of atomic number of Ln in the periodic table. So the difference in the promotion effect of SrF_2 on Ln_2O_3 may be explained by the extent of interaction or ionic exchange between the SrF_2 and Ln_2O_3 phases. It seems that the interaction or ionic exchange between the fluoride and oxide is favored for the Ln_2O_3 with higher lattice oxygen mobility.

For the BaF_2 promoted CeO_2, Tb_4O_7 and Pr_6O_{11}, the C_2 yield of the catalysts ($4BaF_2/CeO_2<8BaF_2/Tb_4O_7<12BaF_2/Pr_6O_{11}$) and high temperature conductivity of the three REOs ($CeO_2<Tb_4O_7<Pr_6O_{11}$) [71] also follow the same sequence, which is consistent with the extent of anionic exchange between BaF_2 and REOs. In the XRD profiles of the three catalysts, small amount of TbOF and relatively large amount of PrOF were detected in the $8BaF_2/Tb_4O_7$ and $12BaF_2/Pr_6O_{11}$ samples, respectively, while no CeOF was detected in $4BaF_2/CeO_2$. The relative concentration of Ln^{4+} ions, which have a strong oxidation ability, on the catalyst's surface also decreased with the increase of high temperature conductivity of the three REOs [60]. These results indicate that the promotion effects of AEF in the REO-based catalysts may be principally related to the extent of phase–phase interaction between fluoride and oxide.

4. Surface acidity/basicity of the fluoride-containing catalyst and their relationship with catalytic property

Many OCM catalysts contain oxides with basic properties such as the oxide of alkali metals, alkaline earth metals and some lanthanides. Therefore, a parallel relationship between catalyst basicity and OCM performance has been suggested [19,72–76]. For some catalyst systems, such a correlation does exist. However, it is now evidenced that a good OCM catalyst need not to be strongly basic, and the relationship between the acidity/basicity and catalytic properties is

complex [47,50–52,57,61,77,78]. For the fluoride-containing REO–AEO-based catalyst system, since the electronegativity of F or the work function of the fluorides is larger than that of O or the oxides, respectively, the presence of F^- may be helpful to decrease the electron donating ability of the catalyst. As a result, a fluoride-containing catalyst will be more favorable than the oxide catalyst to adsorb oxygen in the form of deficiency in electron [51] such as O_2^-. Besides, an AEF/REO catalyst with better OCM performance will be less basic than the corresponding AEO/REO catalyst, which can be sensed by the comparison of CO_2-TPD (temperature-programmed desorption) profiles of BaO/La_2O_3 and BaF_2/La_2O_3 catalysts shown below. Thus an AEF/REO catalyst will be more favorable than the corresponding AEO/REO catalyst to prevent inhibition of CO_2 and to decrease the ignition temperature for the OCM and ODE reactions [51]. These ideas are quite different from the opinion that a good OCM catalyst has to have strong basicity [72–76], but consistent with Lunsford's comments about the influence of Cl^- on the basicity and carbonate formation of the Li^+/MgO system [45–47].

The modification effects of fluoride on the surface oxygen species and acid/base properties of the OCM catalysts have been proved by the XPS (X-ray photoelectron spectroscopy), DRUV (diffuse reflectance ultraviolet) spectra of adsorbed pyridine (Py), CO_2-TPD, and IR (infrared) experiments. XPS experiments (Fig. 1) revealed that, compared to the AEO promoted REO such as SrO/La_2O_3, the surface of an AEF/REO, e.g. SrF_2/La_2O_3, contained more oxygen species with higher binding energy or less negative charge [52,54]. The DRUV spectra of adsorbed pyridine [52] (Fig. 2) and CO_2-TPD (Fig. 3) profiles showed that the surface acidity of a SrF_2/La_2O_3 catalyst, which has better OCM performance than a SrO/La_2O_3, was relatively stronger than that of a SrO/La_2O_3 catalyst. In other words, the SrF_2/La_2O_3 catalyst was less basic than the SrO/La_2O_3 catalyst.

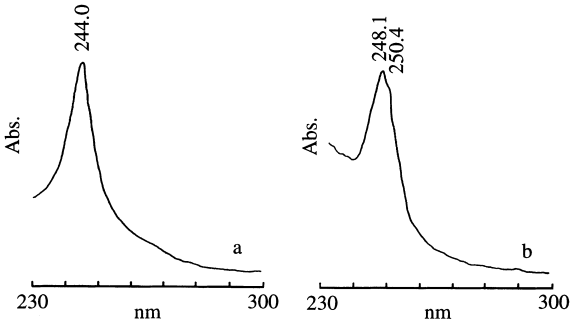

Fig. 2. Diffuse reflectance UV spectra of pyridine adsorbed catalysts: (a) SrO/La_2O_3; (b) SrF_2/La_2O_3 (adapted from Ref. [52]).

The IR spectra of adsorbed CO_2 from 50°C to 750°C recorded over a BaF_2/5.67LaOF catalyst with good catalytic performance for OCM and ODE are shown in Fig. 4. Before taking the IR spectra, the samples were exposed to 1 atm of CO_2 at a chosen temperature for 5 min followed by evacuation to 10^{-3} Torr for 15 min. The results showed that the amount of carbonate in the catalyst first increased with the increase of adsorption temperature, and reached a maximum at about 450°C. With further

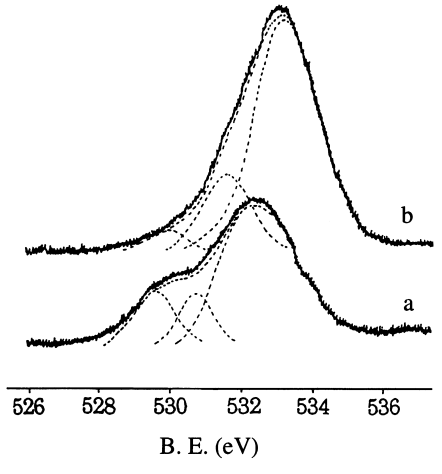

Fig. 1. O1s XPS of O_2-adsorbed (a) SrO/La_2O_3 and (b) $SrF_2La_2O_3$ (adapted from Ref. [52]).

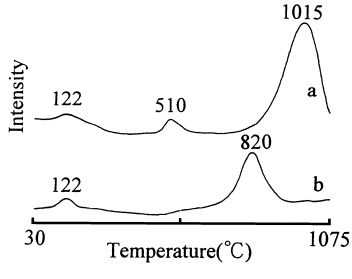

Fig. 3. TPD spectra of CO_2-adsorbed (a) SrO/La_2O_3 and (b) SrF_2/La_2O_3 catalyst.

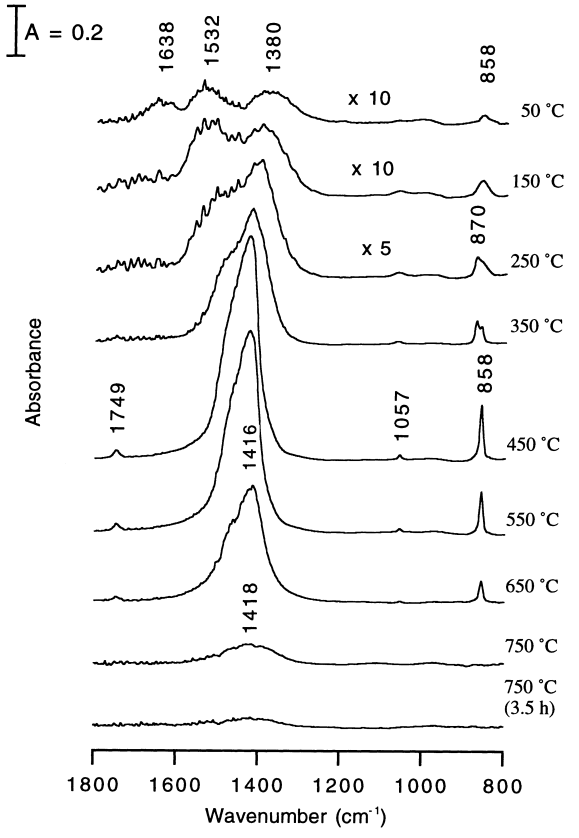

Fig. 4. In situ FTIR spectra of CO_2 adsorption over BaF_2/5.67LaOF sample at various temperatures. (Before taking the spectra, the sample was first exposed to 1 atm of CO_2 at the indicated temperature for 5 min followed by evacuation at the same temperature for 15 min.)

increase of adsorption temperature, the amount of carbonate in the catalyst gradually decreased. As the temperature reached 750°C, there was only a small amount of carbonate remaining in the catalyst. These results provided another experimental evidence which indicated that CO_2 poisoning on the BaF_2/LaOF catalyst under OCM condition was almost negligible.

However, for the pure REO or REOF and the AEF promoted REO or REOF catalysts, the relationship between acid/base properties of the catalysts and their OCM performance is very complicated. As can be seen from the Py-TPD spectra of Y_2O_3 and $2SrF_2$/Y_2O_3 catalysts (Fig. 5) [79], the $2SrF_2/Y_2O_3$ was less acidic than Y_2O_3, and from the CO_2-TPD spectra of La_2O_3, LaOF, $BaF_2/2.33La_2O_3$ and BaF_2/5.67LaOF (Fig. 6), the basicity of BaF_2/5.67LaOF was stronger

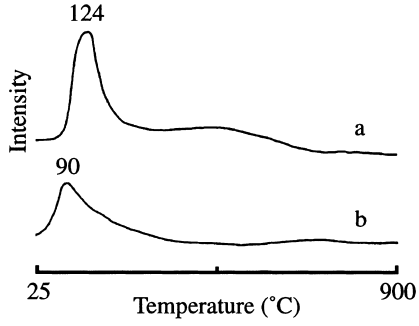

Fig. 5. TPD spectra of Py-adsorbed on (a) Y_2O_3 and (b) $2SrF_2$/Y_2O_3 catalysts (adapted from Ref. [79]).

than that of the LaOF, while the $BaF_2/2.33La_2O_3$ was less basic than La_2O_3. Similar results can also be observed in the CO_2-TPD spectra of the REO with variable valence (CeO_2, Pr_6O_{11} and Tb_4O_7) and the

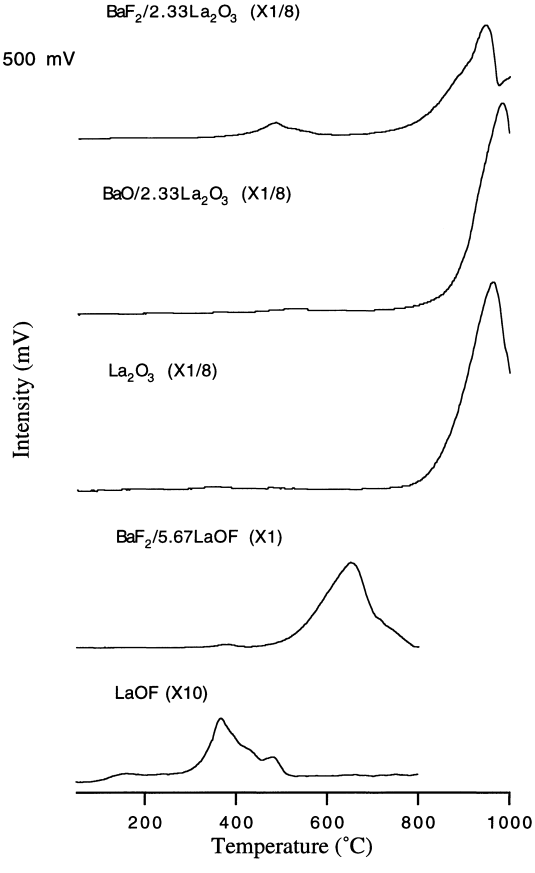

Fig. 6. CO_2-TPD spectra of the catalysts.

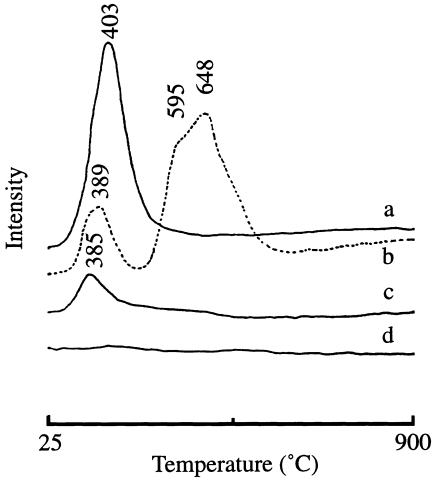

Fig. 7. CO_2-TPD spectra of (a) CeO_2, (b) Pr_6O_{11}, (c) Tb_4O_7 and (d) $4BaF_2/CeO_2$, $12BaF_2/Pr_6O_{11}$, $8BaF_2/Tb_4O_7$ (adapted from Ref. [60]).

BaF_2 promoted CeO_2, Pr_6O_{11} and Tb_4O_7 catalysts (Fig. 7), the catalysts with less basic property demonstrate better OCM performance. These results again indicated that there is no simple correlation between acidity/basicity of an OCM catalyst and its OCM performance.

For an oxide or complex oxide catalyst with stable cation valence, its Lewis basicity, or p-type conductivity, or electron donating ability of lattice oxygen is parallel to its ability of adsorbing and activating oxygen, and to its catalytic activity. However, during the OCM and ODE processes, CO_2 either generated by the side reaction or added to the feed will react instantly with surface Lewis base sites (even with O_2^{2-} species) forming surface carbonate, especially for the catalysts promoted with the oxides of strongly basic property such as BaO, SrO and Li_2O, etc. As a result, the catalyst's ability to adsorb oxygen decreases, while the selectivity improves. Under such circumstances, the activation energy for the reaction increases and the reaction temperature has to be increased in order to maintain a certain activity. For the fluoride-promoted catalyst, besides the anionic vacancies present due to the ionic exchange and/or structurally intrinsic reason, CO_2 usually does not seriously affect the activity of the catalyst. The improvement of selectivity of a fluoride-promoted catalyst may be attributed to the existence of surface fluoride which will isolate the active oxygen species, and the fact that a fluoride modified catalyst will be favorable to adsorb oxygen species in the form less rich in electrons such as O_2^-, which has been known to be much less active than O^- and O_2^{2-}.

Besides the complex relationship between the acid/base property of the catalysts and their catalytic performance, it is worth mentioning that the p-type conductivity is also not a requisite attribute for good OCM catalysts. The experiments of photocurrent measurement with LaOF or BaF_2/9LaOF as working electrode showed that LaOF was a solid electrolyte with "p-type" conductivity. After modifying with 10 mol% of BaF_2, the conductivity of sample BaF_2/9LaOF changed to "n-type" [57]. But for the OCM reaction, BaF_2/9LaOF is a much better catalyst than LaOF (Table 4).

5. Spectroscopic characterization of active oxygen species for OCM

Much attention has been focused on the nature of the active and C_2-selective oxygen species for the OCM reaction. A knowledge of which may help in the search for a better OCM catalyst. For an OCM reaction performed on an oxide or oxyfluoride catalyst with stable cation valence, mono and diatomic anionic species such as O^-, or O_2^{2-}, O_2^- and surface lattice oxygen at low coordination sites have been proposed to be the active oxygen species for the reaction, based on both ex situ and in situ experimental evidences obtained from techniques such as EPR (electron paramagnetic resonance), XPS, IR and Raman spectroscopies [21,48,52,54,57,78,80–84]. Unfortunately, the nature of the oxygen species responsible for the selective conversion of methane to C_2 hydrocarbons has not yet been clarified.

Since 1993, we have been using the in situ IR, Raman and confocal microprobe Raman spectroscopic techniques to characterize oxygen species on SrF_2/La_2O_3 [52], SrF_2/Nd_2O_3 [85], BaF_2/CeO_2 [86], LaOF [87] and BaF_2/LaOF [57,84,87], and catalysts at reaction temperatures. Over the $SrF_2/4La_2O_3$ (Fig. 8), LaOF, BaF_2/5.67LaOF (Fig. 9), SrF_2/Nd_2O_3 (Fig. 10) and $4BaF_2/CeO_2$ (Fig. 11) catalysts, after the samples had been treated with H_2 or evacuated under 10^{-3}–10^{-4} Torr at 700–750°C followed by exposure to O_2, we detected a very clear IR peak at about 1100 cm^{-1}

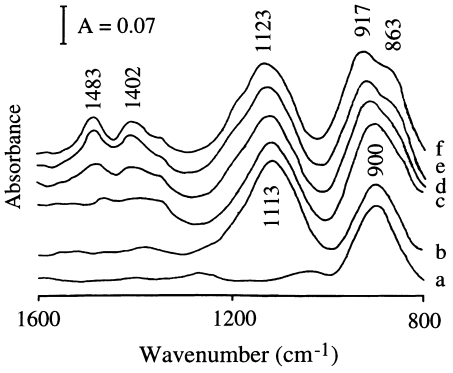

Fig. 8. FTIR spectra of $SrF_2/4La_2O_3$ catalyst: (a) after treatment with H_2 at 700°C, (b)–(f) after exposure to O_2 at 650°C followed by cooling down successively under O_2 to 500°C, 300°C, 100°C and 25°C, respectively (adapted from Ref. [52]).

for the former four catalysts and a Raman peak at 1172 cm^{-1} for $4BaF_2/CeO_2$. The IR bands detected are close to the generally known IR band of adsorbed O_2^- at ca. 1100 cm^{-1}, while the wave number of the Raman band at 1172 cm^{-1} over $4BaF_2/CeO_2$ is close to that of the IR band of adsorbed O_2^- at 1180 cm^{-1} reported by Davydov et al. [88] on O_2-adsorbed TiO_2. Therefore these bands were assigned to a superoxide species (O_2^-). Comparatively, in the Raman experiments performed over some of the alkaline earth–rare earth-based complex oxide (carbonate) catalysts under the similar experimental conditions, the bands of surface O_2^- are usually very weak and can only be detected on a few catalyst systems under the co-feed

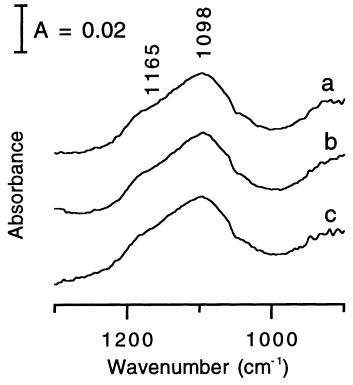

Fig. 9. In situ FTIR spectra of a $BaF_2/5.67LaOF$ sample after exposure to 1 atm of O_2 at 750°C for (a) 1 and (b) 10 min followed by evacuation at the same temperature for (c) 1 min.

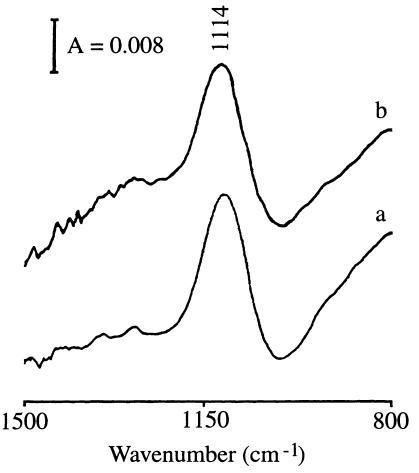

Fig. 10. FTIR spectra of SrF_2/Nd_2O_3 at 700°C: (a) After adsorbing O_2, and (b) followed by purging with He for 15 min.

mode. The possible reason is that the fluoride-containing catalysts have relatively lower electron donating ability, or relatively higher work function, therefore they will be more favorable than the corresponding oxide-based catalysts to adsorb the oxygen in the form of deficiency in electron such as O_2^-. On the other

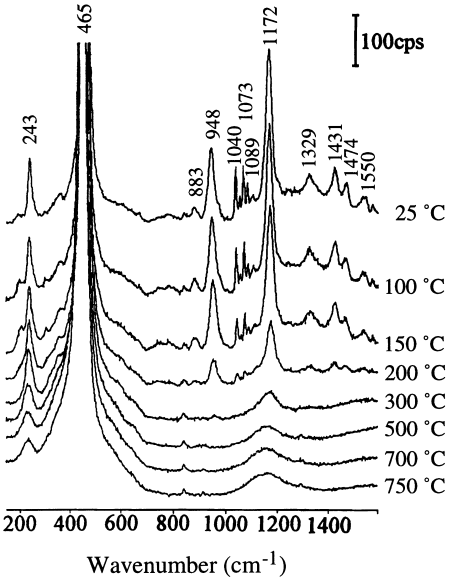

Fig. 11. Microprobe Raman spectra of O_2-pretreated $4BaF_2/CeO_2$ catalyst at the indicated temperature under He atmosphere (adapted from Ref. [86]).

hand, the fluoride-containing catalysts discussed above usually contain large amount of alkaline earth cations with large ionic radii such as Ba^{2+} and Sr^{2+}. Therefore a stronger interaction potential between the single charged superoxide ion and the induced dipole of Ba^{2+} or Sr^{2+} may exist. This is also favorable to the stabilization of O_2^-.

Further IR experiments were carried out to verify the reactivity of assigned O_2^- species with CH_4 under OCM temperature. It was found that at 700–750°C, the O_2^- species on the SrF_2/Nd_2O_3 [85] (Fig. 12), LaOF [87] and BaF_2/5.67LaOF [87] catalysts can react with CH_4 accompanied by the formation of C_2H_4 (at 949–950 cm^{-1} in IR spectroscopy), CO_2 and surface carbonate. Similar results were observed over SrF_2/La_2O_3 catalyst. When an oxygen pre-adsorbed $SrF_2/4La_2O_3$ catalyst was heated at 650°C in a flow of CH_4/O_2=3 for 45 min, the IR band of O_2^- species become weaker and the bands of gas phase C_2H_4, CH_4, CO_2, adsorbed H_2O and surface carbonate were observed [52] (Fig. 13). In another experiment, when a BaF_2/5.67LaOF sample was exposed inside a close sample cell to 1 atm of CH_4/O_2=3.4 at 800°C, a weak IR band of O_2^- at 1098 cm^{-1} and the band of surface carbonate at 850 cm^{-1} were observed immediately. With the increase of exposure time, the bands of surface carbonate grow continuously, while the band of O_2^- increased at the beginning and then decreased, and finally disappeared, probably due to complete consumption of O_2 and removal of O_2^- by the remaining CH_4. During all the period, the peak of gas

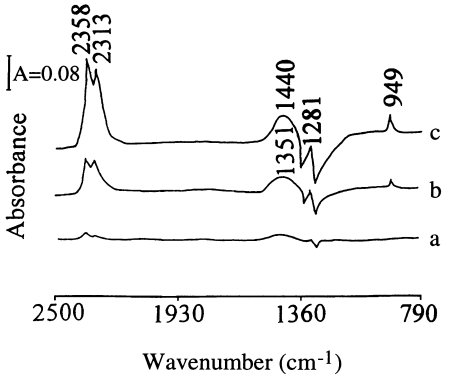

Fig. 12. FTIR spectra recorded during the reaction of CH_4 with O_2-adsorbed SrF_2/Nd_2O_3 at (referenced to the spectra at about 0 min): (a) 5; (b) 15; (c) 30 min.

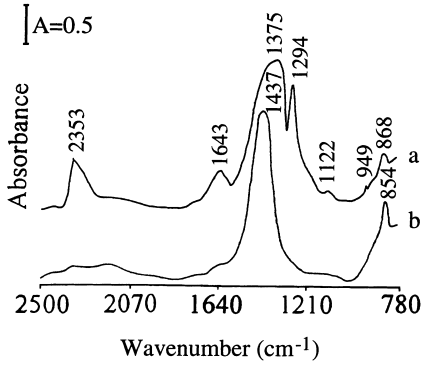

Fig. 13. FTIR spectra of O_2-adsorbed $SrF_2/4La_2O_3$: (a) in CH_4/O_2 (3/1) at 650°C; (b) after purging with He at 650°C (adapted from Ref. [52]).

phase C_2H_4 at 950 cm^{-1} kept increasing. When the above catalyst was switched to a flow of CH_4/O_2=3.4 (15 ml/min), the band of O_2^- was restored gradually (Fig. 14). These results provide direct spectroscopic evidence for the reaction between O_2^- and CH_4 to generate C_2H_4 and side-products under OCM condition, and also provide evidence which indicates that

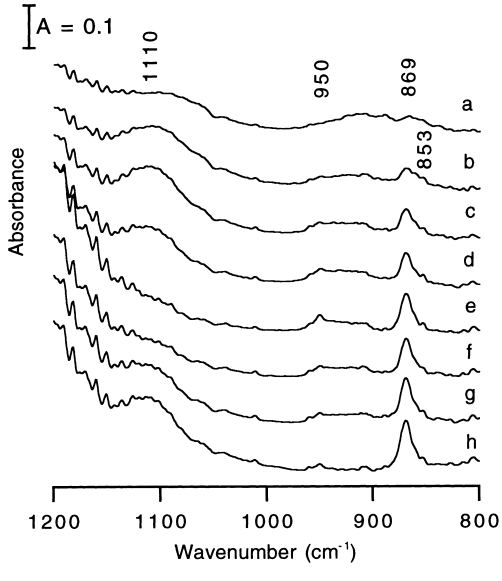

Fig. 14. In situ FTIR spectra of BaF_2/5.67LaOF after exposure to definite amount of CH_4/O_2=3.4 inside a close sample cell at 800°C for (a) 0.5, (b) 1, (c) 3, (d) 5 and (e) 10 min followed by switching to a flow of CH_4O_2=3.4 (15 ml/min) at same temperature for (f) 1, (g) 7 and (h) 12 min.

O_2^- is the active oxygen species or one of the active oxygen species for the OCM reaction over the non-reducible fluoride-containing rare earth-based catalysts such as AEF/REO, AEF/REOF and REOF.

For the catalyst containing rare earth cation with variable valence such as $4BaF_2/CeO_2$, the results of in situ confocal microprobe Raman spectroscopic experiment performed at 750°C show that when an O_2 pre-adsorbed $4BaF_2/CeO_2$ catalyst was heated in a flow of CH_4 at 750°C, the Raman peaks of O_2^- (at 1165 cm^{-1}) and surface lattice oxygen (at 238 and 451 cm^{-1}) species gradually decreased with time in intensities and almost disappeared after ca. 5 and 40 min, respectively (Fig. 15). At 650°C, after switching the CH_4/O_2 (3.4/1) mixture to the above sample which had been adsorbed with O_2 followed by reacting with pure CH_4, the Raman bands of surface lattice oxygen species (at 233 and 449 cm^{-1}) and O_2^- (at 1153 cm^{-1}) reappeared (Fig. 16). When the temperature was increased to 750°C, the Ce–O lattice vibration peak at 449 cm^{-1} was found to decrease slightly, while the other two peaks remained almost unchanged. These observations suggested that both superoxide and lattice oxygen species may be the active oxygen species for the OCM reaction over BaF_2/CeO_2 catalyst system.

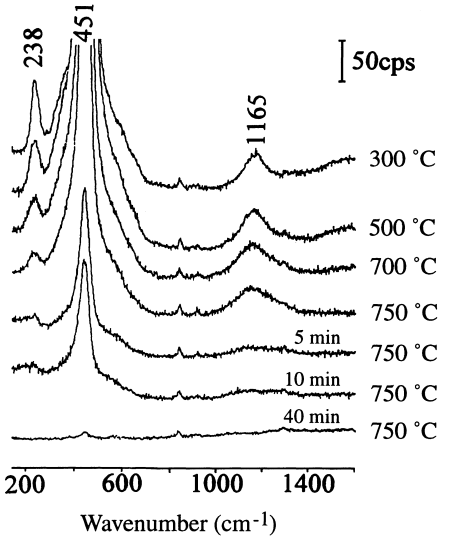

Fig. 15. Microprobe Raman spectra of O_2-pretreated $4BaF_2/CeO_2$ catalyst at the indicated temperature under CH_4 atmosphere (adapted from Ref. [86]).

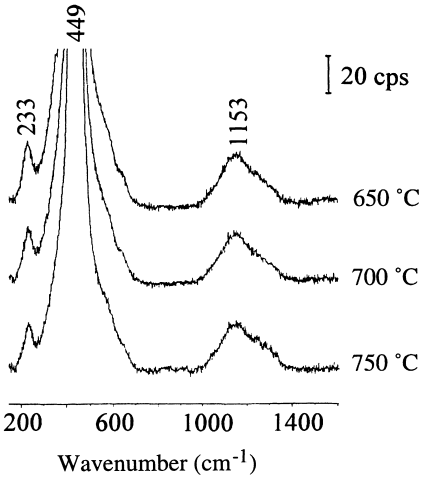

Fig. 16. Microprobe Raman spectra of $4BaF_2/CeO_2$ catalyst at the indicated temperature under CH_4/O_2=3.4 atmosphere (reprinted with permission from Ref. [86]).

On some catalysts, e.g. $4BaF_2/CeO_2$ (Fig. 11), besides the bands related to the Ce–O lattice vibration of CeO_2, the Raman bands of the dioxygen species such as O_2^{2-} (or some sort of the precursor of oxygen species [89]), O_2^{n-} ($1<n<2$) or surface carbonate, O_2^-, $O_2^{\delta-}$ ($0<\delta<1$) and adsorbed O_2 were clearly observed on the surface of O_2-treated sample at room temperature. As the temperature was increased, the Raman peaks of the surface dioxygen species decreased in intensity. At temperatures above 300°C, only the bands of Ce–O lattice vibrations and O_2^- species were detected. A possible reason for the disappearance of "O_2^{2-}" at high temperatures may have resulted from the dissociation of the precursor as mentioned above, because the peroxide species should be more stable than the superoxide species on the REO–AEO-based catalysts.

6. Conclusions

The addition of fluoride such as AEF to the REO (REOF)-based catalyst can significantly improved the catalytic performance for OCM and ODE reactions. The alkali-promoted fluoride-containing REO-based catalysts also demonstrated good catalytic performance for the reactions of ODP and ODIB.

XRD analysis of the fluoride-containing catalysts indicate that partially anionic (O^{2-}/F^-) exchange

between the oxide and the fluoride phases took place in the catalysts, leading to the formation of anionic vacancies and new oxyfluoride phase with defective fluorite structures in the catalyst, promoting the adsorption and activation of oxygen as a result. The improvement in selectivity of a fluoride-promoted catalyst can be attributed to the isolation of active oxygen species by fluoride and to the formation of oxygen species in the form of deficiency in electrons over the fluoride modified catalyst.

An AEF promoted REO catalyst system is less basic than the corresponding AEO promoted REO catalyst system and will therefore be favorable to prevent the CO_2 poisoning. For the OCM reaction, there is no simple correlation between catalytic performance and the acidity/basicity of the catalyst.

In the experiments of in situ spectroscopic characterization of the OCM reaction at the temperature from 650°C to 800°C, O_2^- species were detected over at least five fluoride-containing alkaline earth and/or REO-based OCM catalysts, and the reactions between O_2^- species and CH_4 to form C_2H_4 and the corresponding side-products were observed over four catalysts. These results suggest that O_2^- is the active oxygen species or one of the active species for the OCM reaction over the corresponding catalysts.

Acknowledgements

This work is supported by the National Natural Science Foundation of China, the Key Science and Technology Project and the Doctoral Foundation of Education Committee of China, the Natural Science Foundation of Fujian Province and a grant from SINOPEC. The authors sincerely thank Prof. Y.Y. Liao, Prof. Z.Q. Tian, Mr. X.G. Yan and Ms. P.F. Hong for their kindly help in the experiments and Prof. K.R. Tsai for his instructive suggestions and encouragement.

References

[1] G.E. Keller, M.M. Bhasin, J. Catal. 73 (1982) 9.
[2] F.P. Larkins, M.R. Nordin, Stud. Surf. Sci. Catal. (Methane Conversion) 36 (1988) 406.
[3] J.A. Sofranko, J.J. Leonard, C.A. Jones, A.M. Gaffney, H.P. Withers, Catal. Today 3 (1988) 127.
[4] X. Fang, S. Li, J. Gu, D. Yan, Fenzi Cuihua 6 (1992) 255.
[5] Z. Yu, X. Yang, J.H. Lunsford, M.P. Rosynek, J. Catal. 154 (1995) 163.
[6] W. Hinsen, W. Bytyn, M. Baerns, Proceedings of the Eighth International Congress on Catalysis, vol. 3, Verlag Chemie, Weinheim, 1984, p. 581.
[7] J.P. Bartek, J.M. Hupp, J.F. Brazdil, R.K. Grasselli, Catal. Today 3 (1988) 117.
[8] K. Asami, S. Hashimoto, K. Fujimoto, H. Tominaga, Ind. Eng. Chem. Res. 26 (1987) 1485.
[9] K. Fujimoto, K. Omata, J. Yoshihara, Appl. Catal. 67 (1991) L21.
[10] M.Y. Lo, S.K. Agarwal, G. Marcelin, J. Catal. 112 (1988) 168.
[11] S.K. Agarwal, R.A. Migone, G. Marcelin, Appl. Catal. 53 (1989) 71.
[12] D.J. Driscoll, M. Vilson, J.X. Wang, J.H. Lunsford, J. Am. Chem. Soc. 107 (1985) 58.
[13] T. Ito, J.H. Lunsford, Nature 314 (1985) 721.
[14] J.M. DeBoy, R.F. Hicks, J. Chem. Soc., Chem. Commun. (1988) 982.
[15] S.J. Korf, J.A. Roos, N.A. de Bruijin, J.A. Van Ommen, J.R.H. Ross, Catal. Today 2 (1988) 535.
[16] J.A.S.P. Carriro, G. Follmer, L. Lehmann, M. Baerns, in: M.J. Phillips, M. Ternan (Eds.), Proceedings of the Ninth International Congress on Catalysis, Calgary, 1988, vol. 2, Chem. Inst. Canada, 1988, p. 891.
[17] K. Aika, T. Moriyama, N. Takasaki, E. Iwamatsu, J. Chem. Soc., Chem. Commun. (1986) 1210.
[18] J.A.S.P. Carreriro, M. Baerns, React. Kinet. Catal. Lett. 35 (1987) 349.
[19] T. Ito, T. Tashiro, T. Watanabe, K. Toi, I. Ikemoto, Chem. Lett. (1987) 1723.
[20] J.X. Wang, J.H. Lunsford, J. Phys. Chem. 90 (1986) 5883.
[21] E. Iwamatsu, T. Moriyama, N. Takasaki, K. Aika, J. Chem. Soc., Chem. Commun. (1987) 19.
[22] E. Iwamatsu, T. Moriyama, N. Takasaki, K. Aika, J. Catal. 113 (1988) 25.
[23] J.M. DeBoy, R.F. Hicks, Ind. Eng. Chem. Res. 27 (1988) 1577.
[24] K. Otsuka, Q. Lin, M. Hatano, A. Morikawa, Chem. Lett. (1986) 467.
[25] J. Barrault, M. Grosset, M.H. Aissa, M. Dion, M. Tournoux, Catal. Today 6 (1990) 535.
[26] J.L. Dubois, C.J. Cameron, Chem. Lett. (1991) 1089.
[27] V.R. Choudhary, S.T. Chaudhari, A.M. Rajput, V.H. Rane, Catal. Lett. 3 (1989) 85.
[28] H. Mimoun, A. Robine, S. Bonnaudet, C.J. Cameron, Chem. Lett. (1989) 2185.
[29] V.R. Choudhary, S.T. Chaudhari, A.M. Rajput, V.H. Rane, J. Chem. Soc., Chem. Commun. (1989) 605.
[30] Y. Liu, G. Lin, H. Zhang, K.R. Tsai, Stud. Surf. Sci. Catal. (Natural Gas Conversion II) 81 (1994) 131.
[31] Y. Liu, G. Lin, H. Zhang, J. Cai, H. Wan, K.R. Tsai, Preprints, 203rd ACS Meeting, Div. Fuel Chem. 37 (1992) 356.
[32] E.M. Thorsteinson, T.P. Wilson, F.G. Young, P.H. Kasai, J. Catal. 52 (1978) 116.

[33] A. Guerrero-Ruiz, I. Rodriguez-Ramos, J.L.G. Fierro, V. Soenen, J.M. Herrmann, J.C. Volta, Stud. Surf. Sci. Catal. (New Development in Selective Oxidation by Heterogeneous Catalysis) 72 (1992) 203.
[34] K. Otsuka, K. Jinno, A. Morkawa, J. Chem. Soc., Chem. Commun. (1986) 586.
[35] K. Otsuka, T. Komatsu, Chem. Lett. (1986) 1955.
[36] K. Otsuka, M. Hatano, T. Komatsu, Catal. Today 4 (1989) 409.
[37] A.N. Shigapov, M.A. Novozhilova, S.N. Vereshchagin, A.G. Anshits, V.D. Sokolovskii, React. Kinet. Catal. Lett. 37 (1988) 397.
[38] R. Burch, S. Chalker, P. Louder, D.A. Rice, G. Webb, Appl. Catal. 79 (1991) 265.
[39] K. Fujimoto, S. Hashimoto, K.I. Asami, H. Tominaga, Chem. Lett. (1987) 2157.
[40] B. Wharren, Catal. Today 13 (1992) 311.
[41] D.I. Bradshaw, P.T. Coolen, R.W. Judd, C. Komodromos, Catal. Today 6 (1990) 427.
[42] R.W. Judd, C. Komodromos, T.J. Reynolds, Catal. Today 13 (1992) 237.
[43] T. Ohno, J.B. Moffat, Appl. Catal. A 93 (1993) 141.
[44] S. Ahmed, J.B. Moffat, J. Catal. 121 (1990) 408.
[45] S.J. Conway, J.H. Lunsford, J. Catal. 131 (1991) 513.
[46] S.J. Conway, D.J. Wang, L.H. Lunsford, Appl. Catal. 79 (1991) L1.
[47] J.H. Lunsford, P.G. Hinson, M.P. Rosynek, C. Shi, M. Xu, X. Yang, J. Catal. 147 (1994) 301.
[48] J.H. Lunsford, Angew. Chem., Int. Ed. Engl. 34 (1995) 970.
[49] D.J. Wang, M.P. Rosynek, J.H. Lunsford, J. Catal. 151 (1995) 155.
[50] X.P. Zhou, W.D. Zhang, H.L. Wan, K.R. Tsai, Catal. Lett. 21 (1993) 113.
[51] X.P. Zhou, S.Q. Zhou, W.D. Zhang, Z.S. Chao, W.Z. Weng, R.Q. Long, D.L. Tang, H.Y. Wang, S.J. Wang, J.X. Cai, H.L. Wan, K.R. Tsai, Preprints, 207th ACS Meeting, Div. Petro. Chem. Inc. 39 (1994) 222.
[52] R.Q. Long, S.Q. Zhou, Y.P. Huang, W.Z. Weng, H.L. Wan, K.R. Tsai, Appl. Catal. A 133 (1995) 269.
[53] R.Q. Long, Y.P. Huang, W.Z. Weng, H.L. Wan, K.R. Tsai, Catal. Today 30 (1996) 59.
[54] X.P. Zhou, Z.S. Chao, W.Z. Weng, W.D. Zhang, S.J. Wang, H.L. Wan, K. Tsai, Catal. Lett. 29 (1994) 177.
[55] Z.S. Chao, X.P. Zhou, H.L. Wan, K.R. Tsai, Appl. Catal. A 130 (1995) 127.
[56] X.P. Zhou, Z.S. Chao, J.Z. Luo, H.L. Wan, K.R. Tsai, Appl. Catal. A 133 (1995) 263.
[57] H.L. Wan, Z.S. Chao, W.Z. Weng, X.P. Zhou, J.X. Cai, K.R. Tsai, Catal. Today 30 (1996) 67.
[58] X.P. Zhou, S.Q. Zhou, F.C. Xu, S.J. Wang, W.Z. Weng, H.L. Wan, K.R. Tsai, Chem. Res. Chin. Univ. 9 (1993) 269.
[59] X.P. Zhou, S.Q. Zhou, S.J. Wang, J.X. Cai, W.Z. Weng, H.L. Wan, K.R. Tsai, Chem. Res. Chin. Univ. 9 (1993) 264.
[60] R.Q. Long, J.Z. Luo, M.S. Chen, H.L. Wan, Appl. Catal. A 159 (1997) 171.
[61] S.Q. Zhou, X.P. Zhou, H.L. Wan, K.R. Tsai, Catal. Lett. 20 (1993) 179.
[62] Z.S. Chao, X.P. Zhou, S.J. Wang, F.C. Xu, H.L. Wan, K.R. Tsai, Chin. Chem. Lett. 5 (1994) 685.
[63] W.D. Zhang, X.P. Zhou, D.L. Tang, H.L. Wan, K.R. Tsai, Catal. Lett. 23 (1994) 103.
[64] A. Sher, R. Solomon, K. Lee, M.W. Muller, Phys. Rev. 144 (1966) 593.
[65] B. Delmon, Stud. Surf. Sci. Catal. (Third World Congress on Oxidation Catalysis) 110 (1997) 43.
[66] B. Delmon, P. Ruiz, S.R.G. Carrazán, S. Korili, M.A. Vicent Rodriguez, Z. Sobalik, Stud. Surf. Sci. Catal. (Catalysis in Petroleum Refining and Petrochemical Industries) 100 (1996) 1.
[67] X. Gao, P. Ruiz, Q. Xin, X. Guo, B. Delmon, J. Catal. 148 (1994) 56.
[68] W.D. Zhang, D.L. Tang, X.P. Zhou, H.L. Wan, K.R. Tsai, J. Chem. Soc., Chem. Commun. (1994) 771.
[69] Z.L. Zhang, X.E. Verykios, M. Baerns, Catal. Rev.-Sci. Eng. 36 (1994) 507.
[70] K.A. Gschneidner, Jr., L. Eyring (Eds.), Handbook on the Physics and Chemistry of Rare Earth, vol. 3, Chapter 27, North-Holland, Amsterdam, 1979, p. 385.
[71] Physical Chemistry Constants of Rare Earth, Department of Metals, Zhongshang University, Matallurgial Industry Press, Beijing, 1978, p. 51.
[72] Y. Amenomiya, V.I. Birss, M. Goledzinowski, J. Galuszka, A.R. Sanger, Catal. Rev.-Sci. Eng. 32 (1990) 163.
[73] A.M. Maitra, Appl. Catal. A 104 (1993) 11.
[74] J.A.S.P. Carreiro, M. Baerns, J. Catal. 117 (1989) 258.
[75] A.M. Maitra, I. Campbell, R.J. Tyler, Appl. Catal. A 85 (1992) 27.
[76] V.D. Sokolovskii, S.M. Aliev, O.V. Buyevskaya, A.A. Davydov, Catal. Today 4 (1989) 293.
[77] V.R. Choudhary, V.H. Rane, J. Catal. 130 (1991) 411.
[78] J.H. Lunsford, Stud. Surf. Sci Catal. (Natural Gas Conversion II) 81 (1994) 1.
[79] R.Q. Long, H.L. Wan, Appl. Catal. A 159 (1997) 45.
[80] H. Yamashita, Y. Machida, A. Tomita, Appl. Catal. A 79 (1991) 203.
[81] Y. Osada, S. Koike, T. Fukushima, S. Ogasawara, Appl. Catal. 59 (1990) 59.
[82] Y.D. Liu, H.B. Zhang, G.D. Lin, Y.Y. Liao, K.R. Tsai, J. Chem. Soc., Chem. Commun. (1994) 1871.
[83] R.Q. Long, S.Q. Zhou, Y.P. Huang, H.Y. Wang, H.L. Wan, K.R. Tsai, Chin. Chem. Lett. 6 (1995) 727.
[84] Z.S. Chao, X.P. Zhou, H.L. Wan, K.R. Tsai, Chin. Chem. Lett. 6 (1995) 239.
[85] R.Q. Long, H.L. Wan, H.L. Lai, K.R. Tsai, Gaodeng Xuexiao Huaxue Xuebao 16 (1995) 1796.
[86] R.Q. Long, H.L. Wan, J. Chem. Soc., Faraday Trans. 93 (1997) 355.
[87] W.Z. Weng, M.S. Chen, H.L. Wan, Y.Y. Liao, Catal. Lett. 53 (1998) 43.
[88] A.A. Davydov, M.P. Komarova, V.P. Anufrienko, N.G. Maksimov, Kinet. Katal. 14 (1973) 1519.
[89] Y.D. Liu, H.B. Zhang, G.D. Lin, K.R. Tsai, in: K.R. Tsai, S.Y. Peng (Eds.), Catalysis in C1 Chemistry, Chemical Industry Press, Beijing, 1995, p. 47.